J. Fluid Mech. (1988), *vol.* 192, *pp.* 51–74
Printed in Great Britain

Bragg scattering of water waves by a doubly periodic seabed

By MAMOUN NACIRI AND CHIANG C. MEI
Department of Civil Engineering, Massachusetts Institute of Technology, Cambridge, MA 02139, USA

(Received 17 June 1987)

We extend the recent work on Bragg scattering of water waves by one-dimensional parallel bars of sinusoidal profile to two-dimensional, doubly sinusoidal bed waves. The resonance condition governing the phase matching between the incident, scattered and bed waves is now more complicated and a much richer variety of resonant reflection can occur. In particular, for one normally incident wave there can be two reflected waves forming a standing wave in the transverse direction. Solutions for a wide strip of bed waves are discussed for incident water waves satisfying approximately the Bragg resonance condition. Modifications for a two-dimensional array of hemispheroids are also given. Possible application to the design of submerged breakwaters is suggested.

1. Introduction

During the past decade, the seabed at the Ekofisk oil field in the North Sea has been subsiding at the rate of 40 cm per year (MaCabe 1986). Together with the local waves, this subsidence endangers the drilling platforms during storms. In the past few years, Phillips Petroleum Co. of Norway considered several remedial measures: raising the deck of the platforms, recharging the oil reservoirs with gas and water, or constructing large submerged breakwaters against the prevailing wind waves. The first option was finally chosen and the platforms have now been raised by 6 m.

As a technical challenge, it is worthwhile to examine further the third option and consider an alternative to conventional monolithic breakwaters so as to be better prepared for comparable needs elsewhere. Although the technology of construction is well known, there are disadvantages in putting a large breakwater in some sites. First, large breakwaters transmit large cyclic loads to the supporting soil. Liquefaction, which is a complex effect in soils, can occur to cause foundation failure. Also, in offshore oil fields, complex networks of pipelines are commonly laid on the seabed. A large structure may interfere with the most economical layout and maintenance of pipelines. These difficulties can be significantly reduced if a two-dimensional array of small breakwaters is used instead. In the design of large coastal farms for artificial breeding of fishes, submerged and unobtrusive structures of small dimensions may also be economically more effective and aesthetically appealing.

Recent studies on the Bragg scattering by periodically spaced sand-bars indicate that many small bars can be as effective a breakwater as a single massive structure (Davies & Heathershaw 1984; Mitra & Greenberg 1984; Mei 1985 which contains earlier references; Kirby 1986; Dalrymple & Kirby 1986; Hara & Mei 1987). It is therefore interesting to examine further the effectiveness of a two-dimensional periodic array of breakwaters. To this end much basic physics can be learned from

the study of a doubly sinusoidal seabed. For this geometry some results have been reported by Kirby (1986) based on the numerical solution of an extended mild-slope equation. However, he only performed computations for a strip of bed waves limited in extent in the direction transverse to the incoming waves. In this paper, we shall attempt to examine analytically the details of Bragg resonance over a doubly sinusoidal bed of arbitrary horizontal extent, angle of incidence and constant mean depth. The geometrical optics approximation previously used by Mei will be extended. New energy conservation laws will be derived. The results are then extended to an array of hemispheroids. Extension of the asymptotic equation to slowly varying mean depth will be given in Appendix A.

2. Linearized formulation

As was shown in Mei (1985), the most important physical aspects of Bragg scattering can be learned by assuming the mean depth to be constant; inclusion of bottom slope modifies the results only in quantitative way. We shall limit our analysis to constant mean depth which is assumed to be comparable in order of magnitude to the characteristic wavelength. Extension to a slowly varying mean depth will be made in an Appendix. The linearized governing equations are

$$\nabla^2\phi+\phi_{zz}=0, \quad -h+\epsilon\delta<z<0 \tag{2.1}$$

in the fluid:

$$\phi_{tt}+g\phi_z=0, \quad z=0 \tag{2.2}$$

on the free surface; and

$$\phi_z=\epsilon\nabla\phi\cdot\nabla\delta, \quad z=-h+\epsilon\delta \tag{2.3}$$

on the seabed. The small parameter ϵ is a measure of the steepness of the bed wave and $\epsilon\delta(x, y)$ is the height of the bed wave above the mean bottom. Following Mei (1985), we expect that the uniformly valid description of Bragg resonance requires the consideration of spatial and time ranges much longer than the wave length and wave period. Hence we introduce

$$x_1=\epsilon x, \quad y_1=\epsilon y, \quad t_1=\epsilon t. \tag{2.4}$$

Assuming the multiple-scale expansion

$$\phi=\epsilon\phi^{(1)}+\epsilon^2\phi^{(2)}+O(\epsilon^3) \tag{2.5}$$

and denoting

$$\nabla=\begin{bmatrix}\partial_x\\ \partial_y\end{bmatrix}, \quad \nabla_1=\begin{bmatrix}\partial_{x_1}\\ \partial_{y_1}\end{bmatrix} \tag{2.6}$$

we obtain the following set of perturbation equations: At $O(\epsilon)$

$$\nabla^2\phi^{(1)}+\phi^{(1)}_{zz}=0, \quad -h<z<0, \tag{2.7}$$

$$\phi^{(1)}_{tt}+g\phi^{(1)}_z=0, \quad z=0, \tag{2.8}$$

$$\phi^{(1)}_z=0, \quad z=-h, \tag{2.9}$$

At $O(\epsilon^2)$

$$\nabla^2\phi^{(2)}+\phi^{(2)}_{zz}=-2\nabla\cdot\nabla_1\phi^{(1)}, \quad -h<z<0, \tag{2.10}$$

$$\phi^{(2)}_{tt}+g\phi^{(2)}_z=-2\phi^{(1)}_{tt_1}, \quad z=0, \tag{2.11}$$

$$\phi^{(2)}_z=\nabla\cdot(\delta\nabla\phi^{(1)}), \quad z=-h. \tag{2.12}$$

The formal solution to the first-order problem may be written

$$\phi^{(1)}=\Gamma^+ e^{iS^+}+\Gamma^- e^{iS^-}+\text{c.c.}, \tag{2.13}$$

where S^+ and S^- denote respectively the phases of incident and reflected waves. The frequency ω of both wavetrains is defined by

$$S^+_t=S^-_t=-\omega. \tag{2.14}$$

The wavenumber vectors of the two waves satisfy

$$\nabla S^+=\boldsymbol{k}^+=\begin{bmatrix}\alpha\\ \beta\end{bmatrix}=k\begin{bmatrix}\cos\theta\\ \sin\theta\end{bmatrix}, \tag{2.15}$$

with

$$k=(\alpha^2+\beta^2)^{\frac{1}{2}}=|\boldsymbol{k}^+|=|\boldsymbol{k}^-| \tag{2.16}$$

Note that $\boldsymbol{k}^+$ is given in both magnitude and direction while the direction of $\boldsymbol{k}^-$ under the resonance condition is still to be found. The potential amplitudes of these waves are

$$\Gamma^\pm=-\frac{ig}{\omega}\frac{\cosh k(z+h)}{\cosh kh}\begin{bmatrix}A\\ B\end{bmatrix}, \tag{2.17}$$

with

$$\omega^2=gk\tanh kh. \tag{2.18}$$

The amplitudes A and B are yet unknown. With these results (2.10) and (2.11) become

$$\nabla^2\phi^{(2)}+\phi^{(2)}_{zz}=-\{2\boldsymbol{k}^+\cdot\nabla_1\Gamma^+ e^{iS^+}+2\boldsymbol{k}^-\cdot\nabla_1\Gamma^- e^{iS^-}\}+\text{c.c.}, \quad -h<z<0, \tag{2.19}$$

$$\phi^{(2)}_{tt}+g\phi^{(2)}_z=2i\omega\{\Gamma^+_{t_1} e^{iS^+}+\Gamma^-_{t_1} e^{iS^-}\}+\text{c.c.}, \quad z=0. \tag{2.20}$$

Let the bed wave be described by

$$\begin{aligned}\delta&=D\cos mx\cos ny\\ &=\tfrac{1}{4}D\{e^{i(mx+ny)}+e^{i(mx-ny)}+e^{-i(mx-ny)}+e^{-i(mx+ny)}\}.\end{aligned} \tag{2.21}$$

Each term above may be regarded as a bed wave with zero frequency. The forcing term on the right-hand side of (2.12) is then given by

$$\begin{aligned}\nabla\cdot(\delta\nabla\phi^{(1)})=&-\tfrac{1}{4}D\Gamma^+\boldsymbol{k}^+\cdot\left\{\left[\boldsymbol{k}^+\begin{pmatrix}m\\ n\end{pmatrix}\right]e^{i(mx+ny+S^+)}+\left[\boldsymbol{k}^+\begin{pmatrix}m\\ -n\end{pmatrix}\right]e^{i(mx-ny+S^+)}\right.\\ &\left.+\left[\boldsymbol{k}^+\begin{pmatrix}-m\\ n\end{pmatrix}\right]e^{i(-mx+ny+S^+)}+\left[\boldsymbol{k}^+\begin{pmatrix}-m\\ -n\end{pmatrix}\right]e^{i(-mx-ny+S^+)}\right\}\\ &-\tfrac{1}{4}D\Gamma^-\boldsymbol{k}^-\cdot\left\{\left[\boldsymbol{k}^-\begin{pmatrix}m\\ n\end{pmatrix}\right]e^{i(mx+ny+S^-)}+\left[\boldsymbol{k}^-\begin{pmatrix}m\\ -n\end{pmatrix}\right]e^{i(mx-ny+S^+)}\right.\\ &\left.+\left[\boldsymbol{k}^-\begin{pmatrix}-m\\ n\end{pmatrix}\right]e^{i(-mx+ny+S^-)}+\left[\boldsymbol{k}^-\begin{pmatrix}-m\\ -n\end{pmatrix}\right]e^{i(-mx-ny+S^-)}\right\}, \quad z=-h.\end{aligned} \tag{2.22}$$

3. Condition for Bragg resonance

When any term in the first set of curly brackets of (2.22) has the phase of a free wave solution to the first-order problem, Bragg resonance occurs. The phases of the products are

$$S_1^- = (\alpha-m)x+(\beta-n)y-\omega t, \quad S_2^- = (\alpha+m)x+(\beta-n)y-\omega t, \qquad (3.1a, b)$$

$$S_3^- = (\alpha+m)+(\beta+n)y-\omega t, \quad S_4^- = (\alpha-m)x+(\beta+n)y-\omega t. \qquad (3.1c, d)$$

The corresponding wavenumber vectors are

$$\boldsymbol{k}_1^- = \begin{pmatrix}\alpha-m\\ \beta-n\end{pmatrix}, \quad \boldsymbol{k}_2^- = \begin{pmatrix}\alpha+m\\ \beta-n\end{pmatrix}, \quad \boldsymbol{k}_3^- = \begin{pmatrix}\alpha+m\\ \beta+n\end{pmatrix}, \quad \boldsymbol{k}_4^- = \begin{pmatrix}\alpha-m\\ \beta+n\end{pmatrix}. \qquad (3.2)$$

Clearly when any one of these vectors has magnitude k, that is when any of the following relations holds:

$$(\alpha-m)^2+(\beta-n)^2 = k^2, \quad (\alpha+m)^2+(\beta-n)^2 = k^2, \qquad (3.3a, b)$$

$$(\alpha+m)^2+(\beta+n)^2 = k^2, \quad (\alpha-m)^2+(\beta+n)^2 = k^2, \qquad (3.3c, d)$$

resonance will occur. The wavenumber vector of the resonantly scattered wave will be denoted by $\boldsymbol{k}^-$.

In the Cartesian plane with m, n as the axes, relations (3.3) describe four circles, C_1, C_2, C_3 and C_4, of radius k, centred respectively at (α, β), $(-\alpha, \beta)$ $(-\alpha, -\beta)$ and $(\alpha, -\beta)$. Thus for a given $\boldsymbol{k}^+ = (\alpha, \beta)$, the bed wavenumber vector must end on the circle of radius k centred at the tip of $\boldsymbol{k}^+$, as shown in figure 1. Referring to figure 1, any of the four points

$$P_1\begin{bmatrix}m\\ n\end{bmatrix}, \quad P_2\begin{bmatrix}-m\\ n\end{bmatrix}, \quad P_3\begin{bmatrix}-m\\ -n\end{bmatrix}, \quad P_4\begin{bmatrix}m\\ -n\end{bmatrix}$$

represents the same bed wave. If (3.3a) is satisfied (hence (3.3$b-d$) are not) then the resonantly scattered wave is given by the vector from P_1 to A, or equivalently by $\boldsymbol{OQ}$ which is parallel to $\boldsymbol{P_1A}$. As the topography point P_1 can be anywhere on C_1, all directions are possible for the scattered wave. Alternatively, we can also consider any other P_i, say P_4. Then we must insist that (3.3d) be satisfied. The resonantly reflected wavenumber is still the same $\boldsymbol{k}^-$. As a result, it is sufficient to take just one of the four circles, say C_1. The reflected wave phase S^- is then given by (3.1a).

For P_1 on the circle C_1 with $0 \leqslant \theta \leqslant \frac{1}{2}\pi$, the incident wave has a component in the positive x-direction. For $-\frac{1}{2}\pi \leqslant \psi \leqslant \frac{1}{2}\pi$, the scattered wave is directed to the negative x-direction, partially similar to reflection from long bars parallel to the y-axis. Otherwise, for $\frac{1}{2}\pi \leqslant \psi \leqslant \frac{3}{2}\pi$, the scattered wave is directed to the positive x-direction, partially similar to reflection from long bars parallel to the x-axis. The special case of $\psi = -\theta$ corresponds to long bars parallel to the y-axis, if $-\frac{1}{2}\pi \leqslant \psi \leqslant \frac{1}{2}\pi$; while $\psi = \pi-\theta$ corresponds to long bars parallel to the x-axis, if $\frac{1}{2}\pi \leqslant \psi \leqslant \frac{3}{2}\pi$.

Let us denote the direction of the incident wave with respect to the x-axis by θ, the angle between the incident and reflected waves by φ and the angle between AP and the horizontal axis by ψ. All three angles are taken to be positive if counterclockwise. From now on, we shall refer to ψ as the topography angle as it characterizes the bed waves via

$$m = k(\cos\theta+\cos\psi), \quad n = k(\sin\theta+\sin\psi). \qquad (3.4)$$

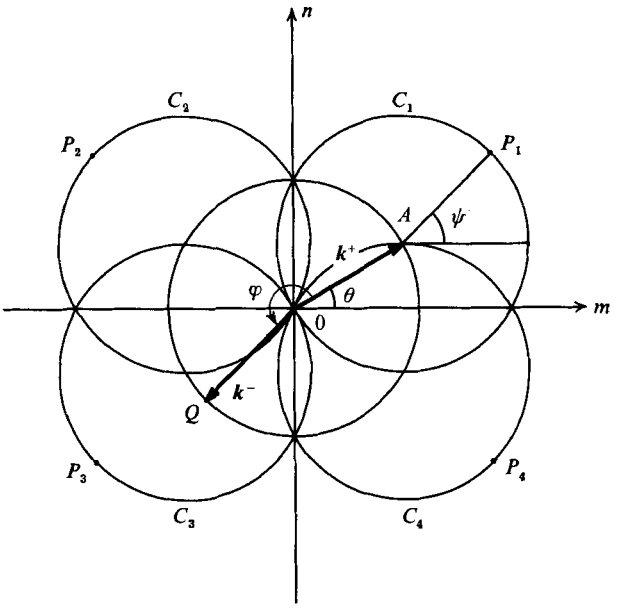

FIGURE 1. Resonance locus, incidence angle = θ, topography angle = ψ.

From figure 1, we infer that

$$\boldsymbol{k}^+\cdot\boldsymbol{k}^- = |\boldsymbol{k}^+|\,|\boldsymbol{k}^-|\cos\varphi = k^2\cos\varphi, \tag{3.5}$$

where

$$\varphi = \psi-\theta-\pi. \tag{3.6}$$

Henceforth, these three angles will be used interchangeably to provide the most compact expressions. Finally we can write

$$\boldsymbol{\nabla}\cdot(\delta\boldsymbol{\nabla}\phi^{(1)}) = -\tfrac{1}{4}D\boldsymbol{k}^+\cdot\boldsymbol{k}^-(\Gamma^-\,\mathrm{e}^{\mathrm{i}S^+}+\Gamma^+\,\mathrm{e}^{\mathrm{i}S^-})+\text{c.c.}+\text{non-resonating terms}, \quad z=-h. \tag{3.7}$$

4. Evolution equations for oblique incidence

Substituting (3.7) into (2.12) and assuming

$$\phi^{(2)} = -\mathrm{i}\gamma^+\,\mathrm{e}^{\mathrm{i}S^+}-\mathrm{i}\gamma^-\,\mathrm{e}^{\mathrm{i}S^-}+\text{c.c.} \tag{4.1}$$

we get from (2.19), (2.20) and (3.5)

$$\gamma^+_{zz}-k^2\gamma^+ = 2\boldsymbol{k}^+\cdot\boldsymbol{\nabla}_1\Gamma^+ + \text{c.c.}, \quad -h<z<0, \tag{4.2}$$

$$\gamma^+_z-\frac{\omega^2}{g}\gamma^+ = -2\frac{\omega}{g}\Gamma^+_{t_1}+\text{c.c.}, \quad z=0, \tag{4.3}$$

$$\gamma^+_z = -\tfrac{1}{4}\mathrm{i}Dk^2\cos\varphi\Gamma^-+\text{c.c.}, \quad z=-h. \tag{4.4}$$

A similar set of equations can be obtained for γ^- by interchanging the superscripts + and −. Solvability for γ^+ and γ^- then gives a set of equations coupling A and B:

$$A_{t_1}+\boldsymbol{C}^+_{\mathrm{g}}\cdot\boldsymbol{\nabla}_1 A = \tfrac{1}{2}\mathrm{i}\Omega_0\cos\varphi B, \tag{4.5a}$$

$$B_{t_1}+\boldsymbol{C}^-_{\mathrm{g}}\cdot\boldsymbol{\nabla}_1 B = \tfrac{1}{2}\mathrm{i}\Omega_0\cos\varphi A. \tag{4.5b}$$

The coupling constant Ω_0 is proportional to the bed-wave slope

$$\Omega_0 = \frac{1}{2}\frac{k\omega D}{\sinh 2kh} \tag{4.6}$$

and has the dimension of frequency. It was pointed out by Mei (1985) that, for parallel bars, Ω_0 defines a frequency band of detuning beyond which Bragg resonance ceases to be effective. The group velocities are given by

$$\boldsymbol{C}_{\mathrm{g}}^{+} = C_{\mathrm{g}}\frac{\boldsymbol{k}^{+}}{k}, \quad \boldsymbol{C}_{\mathrm{g}}^{-} = C_{\mathrm{g}}\begin{pmatrix}\cos(\theta+\varphi)\\ \sin(\theta+\varphi)\end{pmatrix}, \tag{4.7}$$

with

$$C_{\mathrm{g}} = \frac{1}{2}\frac{\omega}{k}\left(1+\frac{2kh}{\sinh 2kh}\right). \tag{4.8}$$

Formally (4.5a, b) are identical to those of Mei (1985) for one-dimensional bars parallel to the y-axis ($n = 0$) except for an extra factor of $\frac{1}{2}$ on the right-hand side of (4.5a, b). To reconcile this, we note that for $n = 0$ the tip of the bed-wave vector must be $(2\alpha, 0)$ which is on both circles C_1 and C_4. In (2.22), both terms in the second line contribute equally to the resonantly reflected waves with phase S^-. Thus we must multiply the right-hand sides of (4.5a, b) by 2; this removes the apparent discrepancy.

5. Evolution equations for normal incidence

When incidence angle $\theta = 0$, the four circles in figure 1 collapse into two: C_1 and C_2, described by

$$C_1: \quad (k-m)^2+n^2 = k^2, \tag{5.1a}$$

$$C_2: \quad (k+m)^2+n^2 = k^2. \tag{5.1b}$$

Since both (m, n) and $(m, -n)$ lie on the circle C_1, there are two reflected waves resonated, as shown in figure 2. Because of symmetry with respect to the m-axis, the sum of the reflected waves is progressive in the negative x-direction but is standing in the y-direction. Thus, three waves with the phases

$$S^+ = kx-\omega t, \quad S_1^- = (k-m)\,x-ny-\omega t, \tag{5.2a, b}$$

$$S_2^- = (k-m)\,x+ny-\omega t \tag{5.2c}$$

resonate each other through the bed wave. The corresponding wavenumber vectors are respectively

$$\boldsymbol{k}^+ = \begin{pmatrix}k\\ 0\end{pmatrix}, \quad \boldsymbol{k}_1^- = \begin{pmatrix}k-m\\ -n\end{pmatrix}, \quad \boldsymbol{k}_2^- = \begin{pmatrix}k-m\\ n\end{pmatrix}. \tag{5.3}$$

Let the first-order potential be of the form

$$\phi^{(1)} = \Gamma^+ \mathrm{e}^{\mathrm{i}S^+} + \Gamma_1^- \mathrm{e}^{\mathrm{i}S_1^-} + \Gamma_2^- \mathrm{e}^{\mathrm{i}S_2^-} + \mathrm{c.c.}, \tag{5.4}$$

where

$$\Gamma^+ = -\frac{\mathrm{i}g}{\omega}\frac{\cosh k(z+h)}{\cosh kh}A, \tag{5.5a}$$

$$\Gamma_{1,2}^- = -\frac{\mathrm{i}g}{\omega}\frac{\cosh k(z+h)}{\cosh kh}B_{1,2}. \tag{5.5b}$$

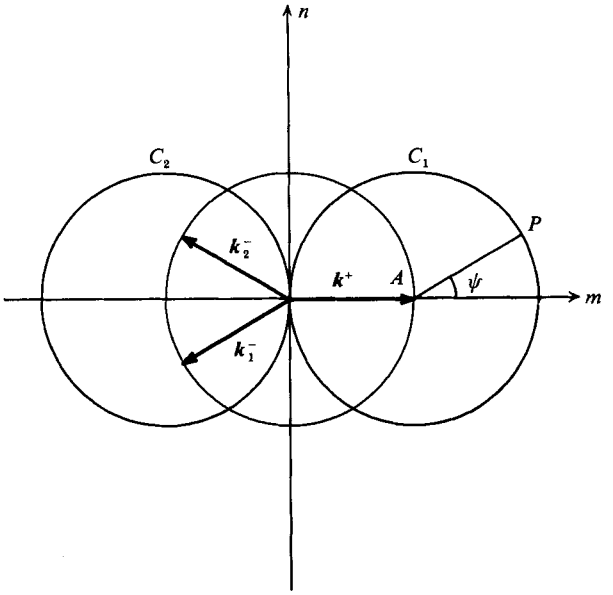

FIGURE 2. Resonance locus, normal incidence with typical standing waves in the y-direction.

With this, the forcing term for the second-order potential is

$$\begin{aligned}\nabla\cdot(\delta\nabla\phi^{(1)}) = -\tfrac{1}{4}D\Gamma^{+}\boldsymbol{k}^{+}\cdot\Bigg\{&\left[\boldsymbol{k}^{+}+\begin{pmatrix}m\\n\end{pmatrix}\right]\mathrm{e}^{\mathrm{i}((k+m)x+ny-\omega t)}+\left[\boldsymbol{k}^{+}+\begin{pmatrix}m\\-n\end{pmatrix}\right]\mathrm{e}^{\mathrm{i}((k+m)x-ny-\omega t)}\\&\times\underline{\left[\boldsymbol{k}^{+}+\begin{pmatrix}-m\\n\end{pmatrix}\right]\mathrm{e}^{\mathrm{i}((k-m)x+ny-\omega t)}}+\underline{\left[\boldsymbol{k}^{+}+\begin{pmatrix}-m\\-n\end{pmatrix}\right]\mathrm{e}^{\mathrm{i}((k-m)x-ny-\omega t)}}\Bigg\}\\-\tfrac{1}{4}D\Gamma_1^{-}\boldsymbol{k}_1^{-}\cdot\Bigg\{&\underline{\left[\boldsymbol{k}_1^{-}+\begin{pmatrix}m\\n\end{pmatrix}\right]\mathrm{e}^{\mathrm{i}(mx+ny+S_1^{-})}}+\left[\boldsymbol{k}_1^{-}+\begin{pmatrix}m\\-n\end{pmatrix}\right]\mathrm{e}^{\mathrm{i}(mx-ny+S_1^{-})}\\&+\left[\boldsymbol{k}_1^{-}+\begin{pmatrix}-m\\n\end{pmatrix}\right]\mathrm{e}^{\mathrm{i}(-mx+ny+S_1^{-})}+\left[\boldsymbol{k}_1^{-}+\begin{pmatrix}-m\\-n\end{pmatrix}\right]\mathrm{e}^{\mathrm{i}(-mx-ny+S_1^{-})}\Bigg\}\\-\tfrac{1}{4}D\Gamma_2^{-}\boldsymbol{k}_2^{-}\cdot\Bigg\{&\left[\boldsymbol{k}_2^{-}+\begin{pmatrix}m\\n\end{pmatrix}\right]\mathrm{e}^{\mathrm{i}(mx+ny+S_2^{-})}+\underline{\left[\boldsymbol{k}_2^{-}+\begin{pmatrix}m\\-n\end{pmatrix}\right]\mathrm{e}^{\mathrm{i}(mx-ny+S_2^{-})}}\\&+\left[\boldsymbol{k}_2^{-}+\begin{pmatrix}-m\\n\end{pmatrix}\right]\mathrm{e}^{\mathrm{i}(-mx+ny+S_2^{-})}+\left[\boldsymbol{k}_2^{-}+\begin{pmatrix}-m\\-n\end{pmatrix}\right]\mathrm{e}^{\mathrm{i}(-mx-ny+S_2^{-})}\Bigg\},\quad z=-h.\end{aligned}\tag{5.6}$$

Clearly, the underlined terms have, in sequence, the phases S_2^{-}, S_1^{-}, S^{+} and S^{+}. Equation (5.6) can be rewritten

$$\nabla\cdot(\delta\nabla\phi^{(1)}) = -\tfrac{1}{2}Dk(k-m)\{\Gamma^{+}(\mathrm{e}^{\mathrm{i}S_1^{-}}+\mathrm{e}^{\mathrm{i}S_2^{-}})+(\Gamma_1^{-}+\Gamma_2^{-})\,\mathrm{e}^{\mathrm{i}S^{+}}\}+\text{c.c.}+\text{non-resonating terms},\quad z=-h.\tag{5.7}$$

Solvability of the second-order problem for $\phi^{(2)}$ then leads to the evolution equations

$$A_{t_1} + \boldsymbol{C}_g^+ \cdot \boldsymbol{\nabla}_1 A = \tfrac{1}{2}\mathrm{i}\Omega_0 \cos\varphi (B_1 + B_2), \tag{5.8a}$$

$$B_{1t_1} + \boldsymbol{C}_{g_1}^- \cdot \boldsymbol{\nabla}_1 B_1 = \tfrac{1}{2}\mathrm{i}\Omega_0 \cos\varphi A, \tag{5.8b}$$

$$B_{2t_1} + \boldsymbol{C}_{g_2}^- \cdot \boldsymbol{\nabla}_1 B_2 = \tfrac{1}{2}\mathrm{i}\Omega_0 \cos\varphi A. \tag{5.8c}$$

The group velocities $\boldsymbol{C}_g^+$, $C_{g_1}^-$ and $C_{g_2}^-$ now have the following components:

$$\boldsymbol{C}_g^+ = C_g \begin{pmatrix} 1 \\ 0 \end{pmatrix}, \tag{5.9a}$$

$$\boldsymbol{C}_{g_1}^- = C_g \begin{pmatrix} -\cos\psi \\ -\sin\psi \end{pmatrix}, \tag{5.9b}$$

$$\boldsymbol{C}_{g_2}^- = C_g \begin{pmatrix} -\cos\psi \\ +\sin\psi \end{pmatrix}, \tag{5.9c}$$

where ψ is the topography angle defined in figure 2. Since $\varphi = \psi - \pi$ for normal incidence, (5.8$a-c$) become

$$A_{t_1} + C_g A_{x_1} = -\tfrac{1}{2}\Omega_0 \cos\psi (B_1 + B_2), \tag{5.10a}$$

$$B_{1t_1} - C_g \cos\psi B_{1x_1} - C_g \sin\psi B_{1y_1} = -\tfrac{1}{2}\mathrm{i}\Omega_0 \cos\psi A, \tag{5.10b}$$

$$B_{2t_1} - C_g \cos\psi B_{2x_1} + C_g \sin\psi B_{2y_1} = -\tfrac{1}{2}\mathrm{i}\Omega_0 \cos\psi A. \tag{5.10c}$$

This set of three coupled equations can be the basis for treating essentially normal incidence with a small inclination away from the x-axis or with a narrow angular spread. For strictly normal incidence, there is no dependence on y_1. The two reflected waves must have identical envelopes,

$$B = B_1 = B_2, \tag{5.11}$$

so that (5.10a–c) are further reduced to

$$A_{t_1} + C_g A_{x_1} = -\mathrm{i}\Omega_0 \cos\psi B, \tag{5.12a}$$

$$B_{t_1} - C_g \cos\psi B_{x_1} = -\mathrm{i}\Omega_0 \cos\psi A. \tag{5.12b}$$

In the limit of one-dimensional bars, $n = 0$ so that $\psi = 0$. The resulting equations again agree with Mei (1985).

In summary, the regions of validity of (4.5a, b) and (5.12a, b) are complementary and do not overlap. Slight detuning is permitted in both of them.

6. Oblique incidence on a wide strip of bed waves

6.1. *Solution to the boundary-value problem*

Assume the doubly periodic bed waves to be confined in the strip $0 < x_1 < L$ where $kL = O(1/\epsilon)$. An incident wavetrain arrives from $x = -\infty$ at an angle θ with the wavenumber

$$\boldsymbol{k} = \boldsymbol{k}^+ + \epsilon \boldsymbol{K}. \tag{6.1}$$

A non-zero $\boldsymbol{K}$ means that the incident wave is slightly detuned from perfect resonance, i.e. from $\boldsymbol{k}^+$, by an amount $\epsilon\boldsymbol{K}$. The corresponding detuning frequency is

$\epsilon\Omega$ with $\Omega = O_g K$ and will be one of the key parameters of the problem. The solutions in various regions may be formally written for $x_1 \leqslant 0$:

$$A = A_0 \exp\{\mathrm{i}K(x_1 \cos\theta + y_1 \sin\theta) - \mathrm{i}\Omega t_1\}; \tag{6.2a}$$

$$B = B_0 \exp\{\mathrm{i}K(-x_1 \cos\theta + y_1 \sin\theta) - \mathrm{i}\Omega t_1\}; \tag{6.2b}$$

for $x_1 \geqslant L$:

$$A = A_1 \exp\{\mathrm{i}K[(x_1 - L)\cos\theta + y_1 \sin\theta] - \mathrm{i}\Omega t_1\}, \tag{6.3a}$$

$$B = 0; \tag{6.3b}$$

and over the bars, $0 \leqslant x_1 \leqslant L$:

$$A = A_0 T(x_1) \exp\{\mathrm{i}Ky_1 \sin\theta - \mathrm{i}\Omega t_1\}, \tag{6.4a}$$

$$B = A_0 R(x_1) \exp\{\mathrm{i}Ky_1 \sin\theta - \mathrm{i}\Omega t_1\}. \tag{6.4b}$$

Upon substituting (6.4a, b) in (4.5a, b), we arrive at the following first-order matrix differential equation:

$$\frac{\mathrm{d}\boldsymbol{X}}{\mathrm{d}\xi} = \mathrm{i}\frac{\Omega_0 L}{C_g}\mathbf{M}\boldsymbol{X}, \tag{6.5$\frac{a}{b}$}$$

where

$$X = [T, R]^{\mathrm{T}}, \tag{6.6}$$

$$\mathbf{M} = \begin{bmatrix} \cos\theta \dfrac{\Omega}{\Omega_0} & \dfrac{1}{2}\dfrac{\cos\varphi}{\cos\theta} \\ \dfrac{1}{2}\dfrac{\cos\varphi}{\cos(\theta+\varphi)} & \dfrac{1-\sin\theta\sin(\theta+\varphi)}{\cos(\theta+\varphi)}\dfrac{\Omega}{\Omega_0} \end{bmatrix} \tag{6.7}$$

and

$$\xi = x_1/L. \tag{6.8}$$

Although (6.5) can also be expressed as a second-order equation for T or R, this matrix form is convenient for extensions in §7. Following standard arguments, we look for homogeneous solutions of the following form:

$$\boldsymbol{X} = \boldsymbol{X}_0 \exp\left(\mathrm{i}\frac{\Omega_0 L}{C_g}\lambda\xi\right). \tag{6.9}$$

Equation (6.5) results in

$$[\mathbf{M} - \lambda\mathbf{I}]\boldsymbol{X}_0 = 0. \tag{6.10}$$

Thus λ is an eigenvalue which is obtained by setting the coefficient determinant to zero:

$$\cos\theta\cos(\theta+\varphi)\lambda^2 - \frac{\Omega}{\Omega_0}\cos\theta\{1-\cos\varphi+2\cos\theta\cos(\theta+\varphi)\}\lambda + \left(\frac{\Omega}{\Omega_0}\right)^2\cos^2\theta\{1-\sin\theta\sin(\theta+\varphi)\} - \tfrac{1}{4}\cos^2\varphi = 0. \tag{6.11}$$

The nature of the eigenvalues is dictated by the characteristic discriminant:

$$\Delta = \left(\frac{\Omega}{\Omega_0}\right)^2\cos^2\theta\{1+\cos(\psi-\theta)\}^2 - \cos^2(\psi-\theta)\cos\theta\cos\psi \tag{6.12}$$

after using (3.6). The angle of incidence θ can be restricted to $[0, \frac{1}{2}\pi]$, i.e. $\cos\theta \geqslant 0$, without any loss of generality. Clearly, the sign of Δ depends on that of $\cos\psi$. Let us first assume that the topography is such that $\cos\psi < 0$, i.e. $\frac{1}{2}\pi \leqslant \psi \leqslant \frac{3}{2}$. The

discriminant Δ is then always positive, implying real eigenvalues and an oscillatory behaviour for R and T, regardless of the magnitude of the detuning Ω/Ω_0. In view of (3.6), the angle of $\boldsymbol{k}^-$, $\theta+\varphi$, is now less than $\frac{1}{2}\pi$ in absolute value. Thus, the scattered wave R is right-going as a result of reflection from a topography which acts almost like long-crested bars parallel to the x-axis.

We next consider $\cos\psi > 0$, i.e. $-\frac{1}{2}\pi \leqslant \psi \leqslant \frac{1}{2}\pi$. For a given incidence θ and topography ψ, the sign of Δ depends on whether the detuning factor Ω/Ω_0 is greater or less than the normalized threshold or cutoff frequency:

$$\frac{\Omega_c}{\Omega_0} \equiv \left(\frac{\cos\psi}{\cos\theta}\right)^{\frac{1}{2}} \left|\frac{\cos(\psi-\theta)}{1+\cos(\psi-\theta)}\right|. \tag{6.13}$$

We define

$$\left(\frac{\Omega}{\Omega_0}\right)^2 \geqslant \left(\frac{\Omega_c}{\Omega_0}\right)^2 \geqslant 0 \tag{6.14a}$$

and

$$0 \leqslant \left(\frac{\Omega}{\Omega_0}\right)^2 \leqslant \left(\frac{\Omega_c}{\Omega_0}\right)^2 \tag{6.14b}$$

to be *supercritical* and *subcritical* detuning respectively. For supercritical (subcritical) detuning, $\Delta \geqslant 0$ ($\Delta \leqslant 0$) and R and T are oscillatory (monotonic) in ξ. The direction of $\boldsymbol{k}^-$ now has a leftward component and the reflection is partially similar to that from long bars parallel to the x-axis.

From (6.10), we solve for the eigenvector corresponding to λ_i:

$$\boldsymbol{X}_i^{\mathrm{T}} = [a_{1i}, a_{2i}] = \left[-\frac{1}{2}\frac{\cos\varphi}{\cos\theta}, \frac{\Omega}{\Omega_0}\cos\theta - \lambda_i\right] \quad (i = 1, 2). \tag{6.15}$$

The general solution for (6.5) is then

$$\begin{bmatrix} T \\ R \end{bmatrix} = \mu_1 \boldsymbol{X}_1 \exp\left[\mathrm{i}\frac{\Omega_0 L}{C_g}\lambda_1\xi\right] + \mu_2 \boldsymbol{X}_2 \exp\left[\mathrm{i}\frac{\Omega_0 L}{C_g}\lambda_2\xi\right] \tag{6.16^a_b}$$

It is shown in Appendix B that continuity of pressure and normal velocity implies $T(0) = 1$ and $R(1) = 0$. From these relations, we obtain the following non-homogeneous linear system for the amplitudes μ_1 and μ_2:

$$\left.\begin{aligned} a_{11}\mu_1 + a_{12}\mu_2 &= 1, \\ a_{21}\mu_1 \exp\left(\mathrm{i}\frac{\Omega_0 L}{C_g}\lambda_1\right) + a_{22}\mu_2 \exp\left[\mathrm{i}\frac{\Omega_0 L}{C_g}\lambda_2\right] &= 0, \end{aligned}\right\} \tag{6.17}$$

which is solved easily. In the supercritical case, the eigenvalues are

$$\lambda_{1\atop 2} = \frac{\cos\theta\,(\Omega/\Omega_0)\,(1-\cos\varphi+2\cos\theta\cos(\theta+\varphi)) \pm \Delta^{\frac{1}{2}}}{2\cos\theta\cos(\theta+\varphi)}. \tag{6.18}$$

Introducing for brevity:

$$S = \frac{\Delta^{\frac{1}{2}}}{2\cos\theta\cos(\theta+\varphi)}, \quad Z = \frac{1-\cos\varphi+2\cos\theta\cos(\theta+\varphi)}{2\cos(\theta+\varphi)} \tag{6.19a, b}$$

we find the reflection and transmission coefficients:

$$R(\xi) = -\frac{\mathrm{i}\cos\varphi}{2\cos(\theta+\varphi)} \frac{\sin[S(\Omega_0 L(1-\xi)/C_g)]\exp[\mathrm{i}Z(\Omega L\xi/C_g)]}{S\cos[S(\Omega_0 L/C_g)] + \mathrm{i}(\Omega/\Omega_0)(Z-\cos\theta)\sin[S(\Omega_0 L/C_g)]} \tag{6.20a}$$

and

$$T(\xi) = \frac{S\cos[S(\Omega_0 L(1-\xi)/C_g)] + \mathrm{i}(\Omega/\Omega_0)(Z-\cos\theta)\sin[S(\Omega_0 L(1-\xi)/C_g)]}{S\cos[S(\Omega_0 L/C_g)] + \mathrm{i}(\Omega/\Omega_0)(Z-\cos\theta)\sin[S(\Omega_0 L/C_g)]} \times\left\{\exp\left[\mathrm{i}Z\frac{\Omega L}{C_g}\xi\right]\right\}. \quad (6.20b)$$

In particular, the reflection intensity along the incident edge of the bar strip is

$$|R(0)|^2 = \frac{[\cos^2\varphi/4\cos^2(\theta+\varphi)]\sin^2[S(\Omega_0 L/C_g)]}{S^2-[\cos^2\varphi/4\cos\theta\cos(\theta+\varphi)]\sin^2[S(\Omega_0 L/C_g)]} \quad (6.21a)$$

and the transmission intensity along the downwave edge is

$$|T(1)|^2 = \frac{S^2}{S^2-[\cos^2\varphi/4\cos\theta\cos(\theta+\varphi)]\sin^2[S(\Omega_0 L/C_g)]}. \quad (6.21b)$$

For the subcritical case, we simply replace $\sin(S(\cdot))$ and $\cos(S(\cdot))$ respectively by $\sinh(|S|(\cdot))$ and $\cosh(|S|(\cdot))$. It can be verified that the scattering coefficients are continuous across the cutoff frequency and are equal to

$$|R(0)|^2 = \frac{[\cos^2\varphi/4\cos^2(\theta+\varphi)](\Omega_0 L/C_g)^2}{1-[\cos^2\varphi/4\cos\theta\cos(\theta+\varphi)](\Omega_0 L/C_g)^2} \quad (6.22a)$$

and

$$|T(1)|^2 = \frac{1}{1-[\cos^2\varphi/4\cos\theta\cos(\theta+\varphi)](\Omega_0 L/C_g)^2}. \quad (6.22b)$$

6.2. *An energy identity*

We first post-multiply the transpose of (6.5) by the complex conjugate of $\boldsymbol{X}$, $\boldsymbol{X}^*$, pre-multiply the conjugate of (6.5) by the transpose of $\boldsymbol{X}$, $\boldsymbol{X}^{\mathrm{T}}$, and then add the two resulting scalar equations:

$$\frac{\mathrm{d}\boldsymbol{X}^{\mathrm{T}}}{\mathrm{d}\xi}\boldsymbol{X}^* + \boldsymbol{X}^{\mathrm{T}}\frac{\mathrm{d}\boldsymbol{X}^*}{\mathrm{d}\xi} = \frac{\mathrm{d}}{\mathrm{d}\xi}[\boldsymbol{X}^{\mathrm{T}}\boldsymbol{X}^*] = \frac{\mathrm{d}}{\mathrm{d}\xi}|\boldsymbol{X}|^2 = \mathrm{i}\frac{\Omega_0 L}{C_g}\boldsymbol{X}^{\mathrm{T}}(\mathbf{M}^{\mathrm{T}}-\mathbf{M})\boldsymbol{X}^*. \quad (6.23)$$

The matrix $[\mathbf{M}^{\mathrm{T}}-\mathbf{M}]$ is easily evaluated from (6.7):

$$\mathbf{M}^{\mathrm{T}}-\mathbf{M} = \tfrac{1}{2}\cos\varphi\left(\frac{1}{\cos(\theta+\varphi)}-\frac{1}{\cos\theta}\right)\begin{bmatrix}0 & 1\\ -1 & 0\end{bmatrix}. \quad (6.24)$$

It follows from (6.23) that

$$\frac{\mathrm{d}}{\mathrm{d}\xi}|\boldsymbol{X}|^2 = \tfrac{1}{2}\mathrm{i}\frac{\Omega_0 L}{C_g}\cos\varphi\left(\frac{1}{\cos(\theta+\varphi)}-\frac{1}{\cos\theta}\right)(TR^*-RT^*). \quad (6.25)$$

Note that both left- and right-hand sides are real. To evaluate the right-hand side, we multiply both sides of (6.5a) by

$$\left(\tfrac{1}{2}R^* - \frac{\Omega}{\Omega_0}\frac{\cos^2\theta}{\cos\varphi}T^*\right)$$

to get

$$\left(\tfrac{1}{2}R^* - \frac{\Omega}{\Omega_0}\frac{\cos^2\theta}{\cos\varphi}T^*\right)\frac{\mathrm{d}T}{\mathrm{d}\xi} = \tfrac{1}{2}\mathrm{i}\frac{\Omega_0 L}{C_g}\frac{\Omega}{\Omega_0}\cos\theta(TR^*-RT^*) + \tfrac{1}{4}\mathrm{i}\frac{\Omega_0 L}{C_g}\frac{\cos\varphi}{\cos\theta}|R|^2 - \mathrm{i}\frac{\Omega_0 L}{C_g}\left(\frac{\Omega}{\Omega_0}\right)^2\frac{\cos^3\theta}{\cos\varphi}|T|^2. \quad (6.26)$$

Taking only the real part, we find

$$\frac{1}{4}\left(R^*\frac{dT}{d\xi}+R\frac{dT^*}{d\xi}\right)-\frac{1}{2}\frac{\Omega}{\Omega_0}\frac{\cos^2\theta}{\cos\varphi}\left(T^*\frac{dT}{d\xi}+T\frac{dT^*}{d\xi}\right)=\tfrac{1}{2}\mathrm{i}\cos\theta\frac{\Omega_0 L}{C_g}\frac{\Omega}{\Omega_0}(TR^*-RT^*). \tag{6.27}$$

Since from (6.5*a*)

$$\left(R^*\frac{dT}{d\xi}+R\frac{dT^*}{d\xi}\right)=\mathrm{i}\cos\theta\frac{\Omega_0 L}{C_g}\frac{\Omega}{\Omega_0}(TR^*-RT^*) \tag{6.28}$$

it follows from (6.27) that

$$\frac{\cos\theta}{\cos\varphi}\frac{d}{d\xi}|T|^2=-\tfrac{1}{2}\mathrm{i}\frac{\Omega_0 L}{C_g}(TR^*-RT^*). \tag{6.29}$$

Finally, upon combining (6.25) and (6.29), we obtain

$$\frac{d}{d\xi}|X|^2=\left(1-\frac{\cos\theta}{\cos(\theta+\varphi)}\right)\frac{d}{d\xi}|T|^2. \tag{6.30}$$

Integrating (6.30) from $\xi=0$ to $\xi=1$ and using the boundary conditions, we find

$$\cos(\theta+\varphi)\,|R(0)|^2+\cos\theta\,(1-|T(1)|^2)=0. \tag{6.31}$$

Thus wave energy flux in the x-direction is conserved. With some algebra, it can be checked that (6.21*a*, *b*) satisfies this energy identity.

6.3. *Numerical results*

In figure 3(*a*) we first present the normalized cutoff frequency as a function of θ and ψ according to (6.13). Along the line $\theta=\frac{1}{2}\pi$, corresponding to glancing incidence, it is singular (the plot has been truncated at the height equal to 2). Along the straight line $\psi=\theta=-\frac{1}{2}\pi$, the cutoff frequency is zero, hence (6.14*a*) holds for all Ω/Ω_0. The solution is thus always supercritical. A sample plot of the reflection coefficient is shown in figure 3(*b*) as a function of Ω/Ω_0 and x_1/L for $\theta=\frac{1}{6}\pi$ and $\psi=\frac{1}{4}\pi$. In this case the normalized cutoff frequency is $\Omega_c/\Omega_0=0.444$. As expected, the greatest reflection at $x=0$ occurs for perfect tuning $\Omega/\Omega_0=0$. For $\Omega/\Omega_0<0.444$, $|R(x)|^2$ decays monotonically in x; for $\Omega/\Omega_0>0.444$, $|R(x)|^2$ is oscillatory. For a fixed x, $|R|^2$ decreases with increasing Ω/Ω_0.

For the same incidence and topography angles $\theta=\frac{1}{6}\pi$ and $\psi=\frac{1}{4}\pi$, we plot on figure 3(*c*) the reflection coefficient at $x=0$ as a function of Ω/Ω_0 and $\Omega_0 L/C_g$, the latter characterizing the slope and extent of bed waves, and decreasing with the normalized water depth. In general $|R(0)|^2$ increases as $\Omega_0 L/C_g$ increases and Ω/Ω_0 decreases. Note that the main lobe of the reflection coefficient corresponds roughly to the subcritical region $\Omega/\Omega_0\leqslant 0.5$. It is evident from figure 3(*c*) that the bed waves can serve as a very effective breakwater provided that tuning is good ($\Omega/\Omega_0\leqslant 0.5$) and the patch of bed waves is wide ($\Omega_0 L/C_g\geqslant 1$).

7. Normal incidence on a wide strip of bed waves

7.1. *The differential system*

We shall now extend the technique developed in §6.1 to solve the boundary-value problem for normal incidence. As a potential solution for (5.10), let us consider a

detuned incident wave with periodic modulation in y_1. Consequently, A, B_1 and B_2 are assumed to be of the following form:

$$\begin{bmatrix} A \\ B_1 \\ B_2 \end{bmatrix} = \begin{bmatrix} T \\ R_1 \\ R_2 \end{bmatrix} e^{iK_2 y_1} e^{-i\Omega t_1}, \tag{7.1}$$

where

$$\boldsymbol{K} = K \begin{bmatrix} \cos\sigma \\ \sin\sigma \end{bmatrix} = \begin{bmatrix} K_1 \\ K_2 \end{bmatrix}, \tag{7.2}$$

and because of nearly normal incidence

$$\Omega = C_g K_1. \tag{7.3}$$

Let us define the sum and difference amplitude coefficients as follows:

$$S = R_1 + R_2 \tag{7.4}$$

and

$$D = R_1 - R_2. \tag{7.5}$$

Upon substituting (7.1) in (5.10*a–c*) and making use of (7.4) and (7.5), we arrive at the following 3×3 matrix differential equation:

$$\frac{d\boldsymbol{X}}{d\xi} = i\frac{\Omega_0 L}{C_g} \mathbf{M} \boldsymbol{X} \tag{7.6}$$

where ξ is still given by (6.8), $\boldsymbol{X}$ and $\mathbf{M}$ are now

$$\boldsymbol{X} = [T, S, D]^T, \tag{7.7}$$

$$\mathbf{M} = \begin{bmatrix} \dfrac{\Omega}{\Omega_0} & -\frac{1}{2}\cos\psi & 0 \\ 1 & -\dfrac{\Omega}{\Omega_0 \cos\psi} & -\dfrac{\Omega}{\Omega_0}\tan\sigma\tan\psi \\ 0 & -\dfrac{\Omega}{\Omega_0}\tan\sigma\tan\psi & -\dfrac{\Omega}{\Omega_0\cos\psi} \end{bmatrix}. \tag{7.8}$$

Use has been made of (7.1), (7.2) and

$$K_2 C_g = \Omega \frac{K_2}{K_1} \equiv \Omega \tan\sigma. \tag{7.9}$$

Since $(k + \epsilon K_1, \epsilon K_2)$ is the actual wavenumber vector of the incident wave, non-zero K_2 means that a small angle of incidence is allowed. Alternatively, one may regard σ as the direction of the incident envelope.

7.2. *The eigenvectors*

We follow the same procedure as in §6.1 and assume a homogeneous solution of the form (6.9). Equation (7.6) yields an eigenvalue problem similar to (6.10). The eigenvalue condition is now a cubic equation:

$$\lambda^3 - \frac{\Omega}{\Omega_0}\left(1 - \frac{2}{\cos\psi}\right)\lambda^2 + \left[\tfrac{1}{2}\cos\psi + \left(\frac{\Omega}{\Omega_0}\right)\right]\left[\frac{1}{\cos^2\psi} - \tan^2\sigma\tan^2\psi - \frac{2}{\cos\psi}\right]\lambda + \frac{1}{2}\frac{\Omega}{\Omega_0} - \left(\frac{\Omega}{\Omega_0}\right)^3\left[\frac{1}{\cos^2\psi} - \tan^2\sigma\tan^2\psi\right] = 0. \tag{7.10}$$

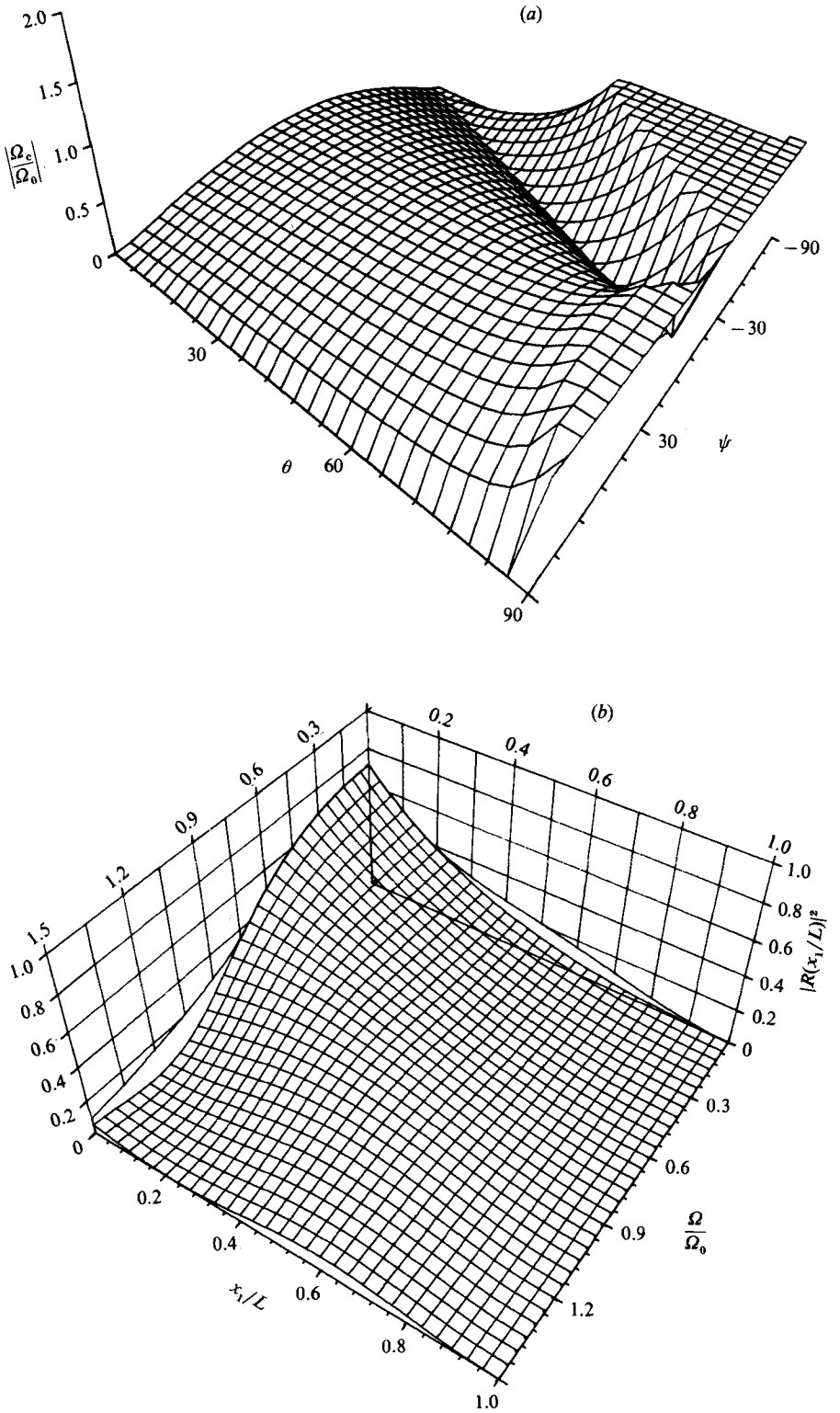

FIGURE 3(*a*, *b*). For caption see facing page.

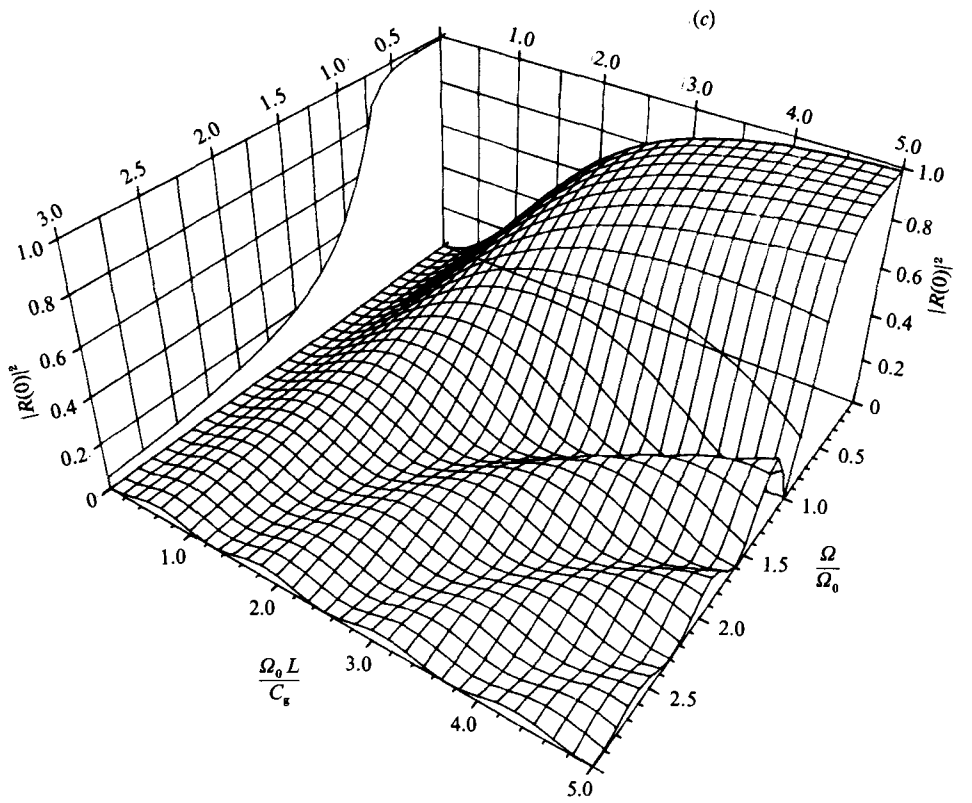

FIGURE 3. (*a*) Cutoff frequency Ω_c/Ω_0 as a function of θ and ψ in degrees. (*b*) $|R|^2$ as a function of location x_1/L and detuning Ω/Ω_0. $\Omega_0 L/C_g = 2$, incidence angle $\theta = \frac{1}{6}\pi$, topography angle $\psi = \frac{1}{4}\pi$. Cutoff frequency is $\Omega_c/\Omega_0 = 0.444$. (*c*) $|R(0)|^2$ as a function of Ω/Ω_0 and $\Omega_0 L/C_g$. $\theta = \frac{1}{6}\pi$ and $\psi = \frac{1}{4}\pi$.

The eigenvalues depend on three parameters: detuning factor Ω/Ω_0, bottom topography angle ψ and incident envelope angle σ; and they are found from (7.10) numerically. The results are displayed in the complex plane of $i\lambda$. It is well known that a third-order polynomial equation with real coefficients has at least one real root, i.e. at least one of the eigenvectors will be purely oscillatory in ξ. The loci of the two other eigenvalues ($i\lambda_i$) are shown in figure 4(*a*, *b*) for a given bottom and two different directions σ of the incident envelope. Consider figure 4(*a*) with $\sigma = 0$. For small detuning, it is seen that $i\lambda$ is predominantly real, thus indicating a monotonic dependence on ξ. However, as Ω/Ω_0 increases, the imaginary part of $i\lambda$ slowly increases while its real part decreases to zero. If detuning is further increased, $i\lambda$ turns sharply after passing the origin and then follows the imaginary axis, implying an oscillatory behaviour in x. This turning point corresponds to the cutoff frequency. Larger detuning causes faster oscillations. While for $\sigma = 0$ the locus has two flat horizontal branches below cutoff, corresponding to purely monotonic behaviour, for $\sigma = \frac{1}{3}\pi$, the locus displays two curved branches reaching the imaginary axis away from the origin, as seen in figure 4(*b*). Thus the effect of σ is to add an oscillatory behaviour to a monotonic trend. It is worth noting that, although successive points correspond to the same increment ($\Delta\Omega/\Omega_0 = 0.2$), they are not evenly spaced in the vicinity of cutoff. Small variations in detuning induce large variations in the eigenvalues.

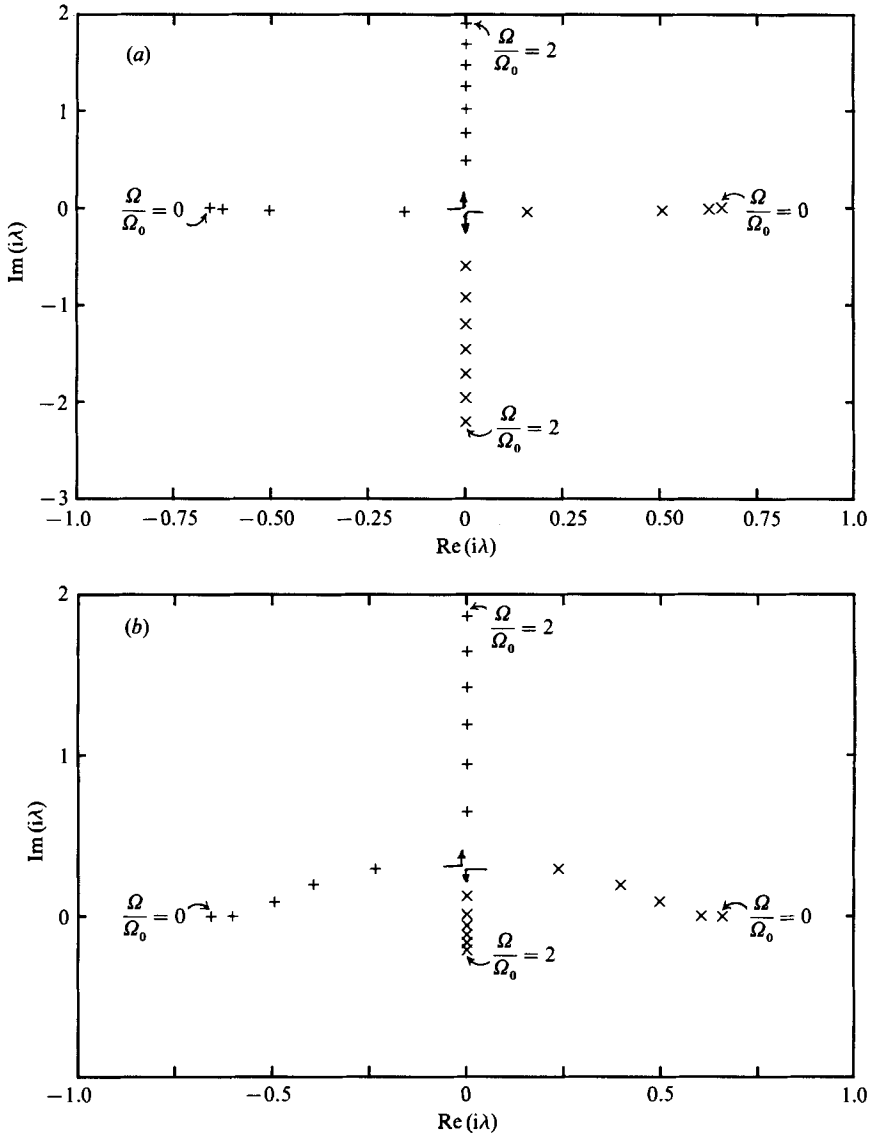

FIGURE 4. Loci of eigenvalues for envelope incidence angle (*a*) $\sigma = 0$ and (*b*) $\sigma = \frac{1}{3}\pi$. Topography angle $\psi = \frac{1}{6}\pi$. Increment $\Delta\Omega/\Omega_0$ between successive symbols is 0.2. × and + represent respectively $i\lambda_1$ and $i\lambda_2$.

We easily obtain the eigenvector corresponding to λ_i:

$$\boldsymbol{X}_i^{\mathrm{T}} = \left[\tfrac{1}{2}\cos\psi\left(\frac{1}{\cos\psi}\frac{\Omega}{\Omega_0}+\lambda_i\right), \left(\frac{\Omega}{\Omega_0}-\lambda_i\right)\left(\frac{1}{\cos\psi}\frac{\Omega}{\Omega_0}+\lambda_i\right), -\left(\frac{\Omega}{\Omega_0}-\lambda_i\right)\frac{\Omega}{\Omega_0}\tan\sigma\tan\psi\right] \quad (i = 1, 2, 3). \tag{7.11}$$

Returning from $[\boldsymbol{X}]^{\mathrm{T}} = [T, S, D]$ to $[\boldsymbol{Y}]^{\mathrm{T}} = [T, R_1, R_2]$, we have

$$\boldsymbol{Y}_i^{\mathrm{T}} = [b_{1i}, b_{2i}, b_{3i}] \quad (i = 1, 2, 3), \tag{7.12}$$

with

$$b_{1i} = \tfrac{1}{2}\cos\psi\left(\frac{1}{\cos\psi}\frac{\Omega}{\Omega_0}+\lambda_i\right), \tag{7.13a}$$

$$b_{2i} = \frac{1}{2}\left(\frac{\Omega}{\Omega_0}-\lambda_i\right)\left[\left(\frac{\Omega}{\Omega_0}\right)\left(\frac{1}{\cos\psi}-\tan\sigma\tan\psi\right)+\lambda_i\right], \tag{7.13b}$$

$$b_{3i} = \frac{1}{2}\left(\frac{\Omega}{\Omega_0}-\lambda_i\right)\left[\left(\frac{\Omega}{\Omega_0}\right)\left(\frac{1}{\cos\psi}+\tan\sigma\tan\psi\right)+\lambda_i\right]. \tag{7.13c}$$

The general solution of the matrix differential equation (7.6) is finally a linear combination of the three eigenmodes:

$$\begin{pmatrix} T \\ R_1 \\ R_2 \end{pmatrix} = \nu_1 Y_1 \exp\left(\mathrm{i}\frac{\Omega_0 L}{C_g}\lambda_1\xi\right)+\nu_2 Y_2 \exp\left(\mathrm{i}\frac{\Omega_0 L}{C_g}\lambda_2\xi\right)+\nu_3 Y_3 \exp\left(\mathrm{i}\frac{\Omega_0 L}{C_g}\lambda_3\xi\right), \tag{7.14}$$

where ν_1, ν_2 and ν_3 are coefficients still to be found through the application of boundary conditions.

7.3. *Solution to the boundary-value problem*

As before, we assume a finite patch in the normalized range $0 \leqslant \xi \leqslant 1$ and $-\infty \leqslant y \leqslant +\infty$. Continuity of pressure and normal velocity at $\xi = 0$ and $\xi = 1$ requires that

$$T(0) = 1, \quad R_1(1) = R_2(1) = 0. \tag{7.15}$$

Equation (7.1) yields the following set of non-homogeneous linear equations:

$$\left.\begin{aligned} \nu_1 b_{11}+\nu_2 b_{12}+\nu_3 b_{13} &= 1, \\ \nu_1 b_{21}\exp\left(\mathrm{i}\frac{\Omega_0 L}{C_g}\lambda_1\right)+\nu_2 b_{22}\exp\left(\mathrm{i}\frac{\Omega_0 L}{C_g}\lambda_2\right)+\nu_3 b_{23}\exp\left(\mathrm{i}\frac{\Omega_0 L}{C_g}\lambda_3\right) &= 0, \\ \nu_1 b_{31}\exp\left(\mathrm{i}\frac{\Omega_0 L}{C_g}\lambda_1\right)+\nu_2 b_{32}\exp\left(\mathrm{i}\frac{\Omega_0 L}{C_g}\lambda_2\right)+\nu_3 b_{33}\exp\left(\mathrm{i}\frac{\Omega_0 L}{C_g}\lambda_3\right) &= 0. \end{aligned}\right\} \tag{7.16}$$

The coefficient determinant can be written as

$$\det = \frac{1}{4}\frac{\Omega}{\Omega_0}\Delta\tan\sigma\tan\psi, \tag{7.17}$$

with

$$\begin{aligned} \Delta = &\left(\frac{1}{\cos\psi}\frac{\Omega}{\Omega_0}+\lambda_1\right)\left(\frac{\Omega}{\Omega_0}-\lambda_2\right)\left(\frac{\Omega}{\Omega_0}-\lambda_3\right)(\lambda_2-\lambda_3)\exp\left[\mathrm{i}\frac{\Omega_0 L}{C_g}(\lambda_2+\lambda_3)\right] \\ &-\left(\frac{1}{\cos\psi}\frac{\Omega}{\Omega_0}+\lambda_2\right)\left(\frac{\Omega}{\Omega_0}-\lambda_1\right)\left(\frac{\Omega}{\Omega_0}-\lambda_3\right)(\lambda_1-\lambda_3)\exp\left[\mathrm{i}\frac{\Omega_0 L}{C_g}(\lambda_1+\lambda_3)\right] \\ &+\left(\frac{1}{\cos\psi}\frac{\Omega}{\Omega_0}+\lambda_3\right)\left(\frac{\Omega}{\Omega_0}-\lambda_2\right)\left(\frac{\Omega}{\Omega_0}-\lambda_1\right)(\lambda_1-\lambda_2)\exp\left[\mathrm{i}\frac{\Omega_0 L}{C_g}(\lambda_1+\lambda_2)\right]. \end{aligned} \tag{7.18}$$

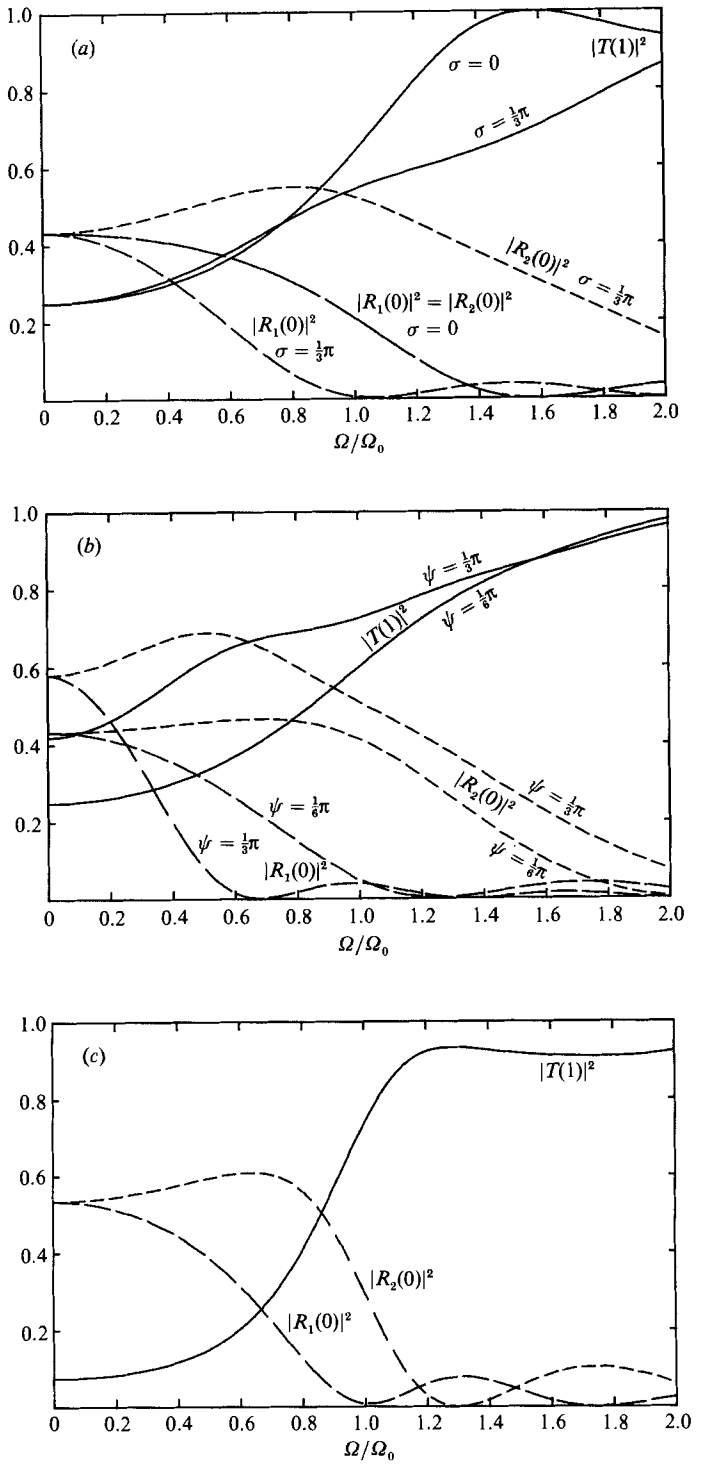

FIGURE 5. Scattering coefficients as a function of Ω/Ω_0 for (*a*) $\Omega_0 L/C_g = 2$, topography angle $\psi = \frac{1}{6}\pi$, envelope incidence $\sigma = 0$, $\sigma = \frac{1}{3}\pi$; (*b*) $\Omega_0 L/C_g = 2$, topography angle $\psi = \frac{1}{6}\pi$, $\psi = \frac{1}{3}\pi$, envelope incidence $\sigma = \frac{1}{4}\pi$; (*c*) $\Omega_0 L/C_g = 3$, topography angle $\psi = \frac{1}{6}\pi$, envelope incidence $\sigma = \frac{1}{6}\pi$. $|T(1)|^2$ (——), $|R_1(0)|^2$ (— — —) and $|R_2(0)|^2$ (– – –).

After some algebra we find

$$\nu_1 = \frac{2}{\Delta \cos\psi}\left(\frac{\Omega}{\Omega_0}-\lambda_2\right)\left(\frac{\Omega}{\Omega_0}-\lambda_3\right)(\lambda_2-\lambda_3)\exp\left[\mathrm{i}\frac{\Omega_0 L}{C_g}(\lambda_2+\lambda_3)\right], \tag{7.19a}$$

$$\nu_2 = \frac{2}{\Delta \cos\psi}\left(\frac{\Omega}{\Omega_0}-\lambda_1\right)\left(\frac{\Omega}{\Omega_0}-\lambda_3\right)(\lambda_3-\lambda_1)\exp\left[\mathrm{i}\frac{\Omega_0 L}{C_g}(\lambda_1+\lambda_3)\right] \tag{7.19b}$$

and

$$\nu_3 = \frac{2}{\Delta \cos\psi}\left(\frac{\Omega}{\Omega_0}-\lambda_1\right)\left(\frac{\Omega}{\Omega_0}-\lambda_2\right)(\lambda_1-\lambda_2)\exp\left[\mathrm{i}\frac{\Omega_0 L}{C_g}(\lambda_1+\lambda_2)\right] \tag{7.19c}$$

The three amplitudes are now fully determined by (7.1) and (7.14).

7.4. *The limit of zero detuning*

When $\Omega/\Omega_0 = 0$, the last row of the matrix $\mathbf{M}$ in (7.8) vanishes, hence $D = 0$. As a consequence, we can reduce (7.6) to

$$\frac{\mathrm{d}}{\mathrm{d}\xi}\begin{bmatrix}T\\S\end{bmatrix} = \mathrm{i}\frac{\Omega_0 L}{C_g}\begin{bmatrix}0 & -\frac{1}{2}\cos\psi\\ 1 & 0\end{bmatrix}\begin{bmatrix}T\\S\end{bmatrix}. \tag{7.20}$$

After solving the boundary-value problem, we find the reflected and transmitted wave amplitudes to be

$$R_1 = R_2 = -\tfrac{1}{2}\mathrm{i}\,\frac{1}{(\frac{1}{2}\cos\psi)^{\frac{1}{2}}}\,\frac{\sinh\left[\dfrac{\Omega_0 L}{C_g}(\frac{1}{2}\cos\psi)^{\frac{1}{2}}(1-\xi)\right]}{\cosh\left[\dfrac{\Omega_0 L}{C_g}(\frac{1}{2}\cos\psi)^{\frac{1}{2}}\right]} \tag{7.21a}$$

and

$$T = \frac{\cosh\left[\dfrac{\Omega_0 L}{C_g}(\frac{1}{2}\cos\psi)^{\frac{1}{2}}(1-\xi)\right]}{\cosh\left[\dfrac{\Omega_0 L}{C_g}(\frac{1}{2}\cos\psi)^{\frac{1}{2}}\right]}. \tag{7.21b}$$

7.5. *Numerical results*

In figure 5(*a*) we show the reflection and transmission coefficients for a fixed bottom topography with $\Omega_0 L/C_g = 2$, for $\sigma = 0$ and $\frac{1}{3}\pi$. For perfectly normal incidence ($\sigma = 0$), the reflection is symmetrical, $R_1(0) = R_2(0)$. Note that, for perfect tuning, the amplitude incidence angle does not affect the scattering coefficients and reflection is symmetrical about the x-axis, as expected. However, when $\sigma = \frac{1}{3}\pi$ more reflection is directed towards positive y. Although the sum $|R_1(0)|^2$ and $|R_2(0)|^2$ is maximum for perfect tuning $\Omega/\Omega_0 = 0$, $|R_2(0)|^2$ reaches a maximum for non-zero detuning ($\Omega/\Omega_0 \approx 0.9$). From figure 4(*b*), we can infer that the cutoff frequency lies around 0.9. Figure 5(*a*) shows very clearly, for $\sigma = \frac{1}{3}\pi$, how both $|R_2(0)|$ and $|T(1)|$ are neither purely oscillatory nor purely monotonic for $\Omega/\Omega_0 \leqslant 0.9$, as should be expected from the eigenvalue loci.

Consider now figure 5(*b*), where $\sigma = \frac{1}{4}\pi$. Change of topography from $\psi = \frac{1}{6}$ to $\frac{1}{3}\pi$ induces drastic changes in R_1, R_2 and T. Finally, in figure 5(*c*), we let $\Omega_0 L/C_g$ be increased to 3. Reflection is now greatly enhanced, while transmission is sharply decreased, especially below cutoff. The oscillatory behaviour above cutoff is evident.

Similar to the case of oblique incidence, the following energy identity relating the scattering coefficients can be derived (see Appendix C):

$$\cos\psi(|R_1(0)|^2+|R_2(0)|^2)+|T(1)|^2=1. \tag{7.22}$$

This conservation law has been used to check our numerical results.

8. Doubly periodic array of hemispheroids

To see the potential of doubly periodic structures as breakwaters, it is necessary to examine configurations that can be mass produced and easily installed. Hemispheroids are probably the simplest of such configurations. Theoretically, the slope along the base is too large to be compatible with the approximation used here. It is however worthwhile to ignore this local inconsistency in order to have a crude estimation of the effectiveness of such structures. Because of periodicity in the short scales, the bed topography above the mean depth can be expanded as

$$\delta(x, y, x_1, y_1)=\sum_{p=-\infty}^{+\infty}\sum_{q=-\infty}^{+\infty}\tfrac{1}{4}D_{pq}(x_1, y_1)\,\mathrm{e}^{\mathrm{i}mpx}\,\mathrm{e}^{\mathrm{i}nqy}. \tag{8.1}$$

Recall from (2.3) that $\epsilon\delta$ is the height of the structure. Note that m and n are wavenumbers and D_{pq} can depend on the slow scales x_1 and y_1. Clearly, the resonant terms correspond to $p=\pm1$ and $q=\pm1$. Again it suffices to consider D_{11} which corresponds to the circle C_1 in figure 1.

Consider a lattice of half-spheroids spaced in the x- and y-directions at distances $\mathscr{L}$ and ℓ respectively. Thus

$$\mathscr{L}=2\pi/m, \quad \ell=2\pi/n. \tag{8.2}$$

The physical height of each spheroid is ϵa and the radius of the circular base is a so that

$$\delta(x, y)=\begin{cases}(a^2-x^2-y^2)^{\frac{1}{2}} & \text{if } x^2+y^2\leqslant a^2\\ 0 & \text{if } x^2+y^2>a^2, \quad |x|<\tfrac{1}{2}\mathscr{L}, \quad |y|<\tfrac{1}{2}\ell\end{cases} \tag{8.3}$$

and is periodic over $\mathscr{L}$ by ℓ rectangles. The Fourier coefficients are

$$\tfrac{1}{4}D_{11}\mathscr{L}\ell=\int_{-\frac{1}{2}\mathscr{L}}^{\frac{1}{2}\mathscr{L}}\mathrm{d}x\int_{-\frac{1}{2}\ell}^{\frac{1}{2}\ell}\mathrm{d}y\,\delta(x, y)\,\mathrm{e}^{-\mathrm{i}mx}\,\mathrm{e}^{-\mathrm{i}ny} \tag{8.4}$$

or

$$D_{11}=\frac{mn}{\pi^2}a^3\int_0^1\mathrm{d}u\,u(1-u^2)^{\frac{1}{2}}\int_0^{2\pi}\mathrm{d}\gamma\,\mathrm{e}^{\mathrm{i}ua(m\cos\gamma+n\sin\gamma)} \tag{8.5}$$

after transforming to polar coordinates. In the inner integral

$$\mathscr{I}=\int_0^{2\pi}\mathrm{d}\gamma\,\mathrm{e}^{\mathrm{i}ua(m\cos\gamma+n\sin\gamma)} \tag{8.6}$$

the exponent can be written as

$$2iuka\sin\tfrac{1}{2}\varphi\sin(\gamma-\theta-\tfrac{1}{2}\varphi). \tag{8.7}$$

Letting

$$z=2uka\sin\tfrac{1}{2}\varphi \tag{8.8}$$

we get

$$\mathscr{I}=\int_0^{2\pi}\mathrm{d}\gamma\,[\cos(z\sin(\gamma-\theta-\tfrac{1}{2}\varphi))+\mathrm{i}\sin(z\sin(\gamma-\theta-\tfrac{1}{2}\varphi))]. \tag{8.9}$$

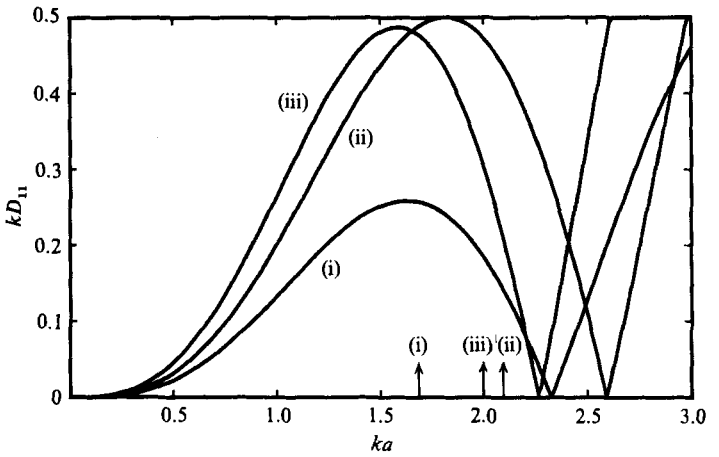

FIGURE 6. Relation between ka and the equivalent slope of the double sinusoid, kD_{11}. (i) $\theta = 0$, $\psi = \frac{1}{6}\pi$; (ii) $\theta = 0$, $\psi = \frac{1}{3}\pi$ and (iii) $\theta = \frac{1}{6}\pi$, $\psi = \frac{1}{4}\pi$.

Making use of the following formulae:

$$\cos(z\sin t) = J_0(z) + 2\sum_{j=1}^{\infty} J_{2j}(z)\cos 2jt, \tag{8.10a}$$

$$\sin(z\sin t) = 2\sum_{j=1}^{\infty} J_{2j+1}(z)\sin(2j-1)t \tag{8.10b}$$

and the orthogonality of trigonometric functions, we find

$$\mathscr{I} = 2\pi J_0(2uka\sin(\tfrac{1}{2}\varphi)). \tag{8.11}$$

This enables us to evaluate D_{11} explicitly from (8.5)

$$D_{11} = mna^3\left(\frac{2}{\pi}\right)^{\frac{1}{2}} Q^{-\frac{3}{2}} J_{\frac{3}{2}}(Q) = \frac{2}{\pi} mna^3 Q^{-3}(\sin Q - Q\cos Q), \tag{8.12}$$

where
$$Q = 2ka\sin(\tfrac{1}{2}\varphi) = -2ka\cos[\tfrac{1}{2}(\psi-\theta)], \tag{8.13}$$

and, in view of (3.4),

$$m = k(\cos\theta + \cos\psi), \quad n = k(\sin\theta + \sin\psi). \tag{8.14}$$

In order to prevent neighbouring hemispheroids from contact, the normalized radius must satisfy

$$ka \leqslant \min(\tfrac{1}{2}k\mathscr{L}, \tfrac{1}{2}k\ell). \tag{8.15}$$

The quantity ϵkD_{11} can be regarded as the slope of the equivalent doubly sinusoidal seabed. Figure 6 shows the dependence of kD_{11} on the normalized radius of the circular base ka, for various incidence angles θ and topography angles ψ. The vertical arrows represent the upper bounds of ka allowed by (8.15). Clearly, there is a optimum radius for which kD_{11} and hence the reflection is the greatest. The extremum is easily found to be at

$$ka = \frac{\frac{1}{2}\pi}{|\sin(\frac{1}{2}\varphi)|} = O(1), \tag{8.16}$$

which always satisfy (8.15). Although $ka = O(1)$, the small height of the structure ϵa implies that the volumes of both a half-spheroid and one period of the sinusoidal corrugation are comparable. Since half-spheroids are likely to be easier to install on a flat bottom, they can serve as an effective breakwater, if properly arranged.

We thank the financial support of US Office of Naval Research, Ocean Engineering Division through Contract N00014-83K-0550, NR294095 and that of the US National Science Foundation through Grant (MSM8514919). This study was motivated by conversations between Dr Even Mehlum of Norwave, Oslo, and C.C.M. in 1985.

Appendix A. Approximate equations for slowly varying mean depth

Let the mean depth be $h(x_1, y_1)$. The incident phase function reads

$$S^+ = \int^x \alpha(x_1, y_1)\,\mathrm{d}x + \int^y \beta(x_1, y_1)\,\mathrm{d}y - \omega t. \tag{A 1}$$

We consider a slowly varying, doubly sinusoidal topography defined as follows:

$$\delta = D\cos\left\{\int^x m(x_1, y_1)\,\mathrm{d}x\right\}\cos\left\{\int^y n(x_1, y_1)\,\mathrm{d}y\right\}. \tag{A 2}$$

Bragg resonance is still governed by one of equations (3.3). Solvability conditions at the second order lead finally to the coupled equations. For general oblique incidence, one only needs to add the term $\frac{1}{2}A^{\pm}\nabla_1\cdot\boldsymbol{C}_g^{\pm}$ to the left-hand side of equations (4.5^{a}_{b}) respectively. For nearly normal incidence, one needs to add $\frac{1}{2}A\nabla_1\cdot\boldsymbol{C}_g^{+}$ and $\frac{1}{2}B_{1,2}\nabla_1\cdot\boldsymbol{C}_{g_{1,2}}^{-}$ to the left-hand side of (5.8*a–c*) respectively.

Appendix B. Derivation of boundary conditions

The expressions of the wave potential in the various regions are

$$\phi_< = -\frac{\mathrm{i}g}{\omega}\{\mathrm{e}^{\mathrm{i}S^+} + R\,\mathrm{e}^{\mathrm{i}S^-}\}\frac{\cosh k(z+h)}{\cosh kh} \tag{B 1a}$$

to the left of topography, $x < 0$;

$$\phi = -\frac{\mathrm{i}g}{\omega}\{A\,\mathrm{e}^{\mathrm{i}S^+} + B\,\mathrm{e}^{\mathrm{i}S^-}\}\frac{\cosh k(z+h)}{\cosh kh} \tag{B 1b}$$

over the topography, $0 \leqslant x \leqslant L/\epsilon$;

$$\phi_> = -\frac{\mathrm{i}g}{\omega}T\,\mathrm{e}^{\mathrm{i}S^+}\frac{\cosh k(z+h)}{\cosh kh} \tag{B 1c}$$

to the right of topography, $x \geqslant L/\epsilon$. Continuity of pressure implies that

$$\phi_{<,t} = \phi_{,t} \quad \text{at } x = 0; \quad \phi_{,t} = \phi_{>,t} \quad \text{at } x = L/\epsilon, \tag{B 2}$$

which reduces to

$$\mathrm{e}^{\mathrm{i}ky\sin\theta}(1 - A(0)) + \mathrm{e}^{\mathrm{i}ky\sin(\theta+\varphi)}(R - B(0)) = 0 \tag{B 3a}$$

and

$$\mathrm{e}^{\mathrm{i}k[L\cos\theta/\epsilon + y\sin\theta]}(A(L) - T) + \mathrm{e}^{\mathrm{i}k[L\cos(\theta+\varphi)/\epsilon + y\sin(\theta+\varphi)]}B(L) = 0. \tag{B 3b}$$

Similarly, continuity of velocities reads

$$\phi_{<,x} = \phi_{,x} \quad \text{at } x = 0; \quad \phi_{,x} = \phi_{>,x} \quad \text{at } x = L/\epsilon. \tag{B 4}$$

Upon using (B 1), we obtain

$$\cos\theta\, \mathrm{e}^{\mathrm{i}ky\sin\theta}(1-A(0)) + \cos(\theta+\varphi)\, \mathrm{e}^{\mathrm{i}ky\sin(\theta+\varphi)}(R-B(0)) = 0 \tag{B 5a}$$

and

$$\cos\theta\, \mathrm{e}^{\mathrm{i}k[L\cos\theta/\epsilon+y\sin\theta]}(A(L)-T) + \cos(\theta+\varphi)\, \mathrm{e}^{\mathrm{i}k[L\cos(\theta+\varphi)/\epsilon+y\sin(\theta+\varphi)]}B(L) = 0. \tag{B 5b}$$

In order to satisfy (B 3*a*, *b*) and (B 5*a*, *b*) for all y, we have to set the coefficient of all y-dependent exponentials to zero, leading to

$$A(0) = 1, \quad R = B(0) \tag{B 6a}$$

and

$$A(L) = T, \quad B(L) = 0. \tag{B 6b}$$

Appendix C. Energy conservation law for normal incidence

Following the procedure leading to (6.23), we obtain from (7.6) a similar result with

$$\mathbf{M}^{\mathrm{T}} - \mathbf{M} = (1+\tfrac{1}{2}\cos\psi)\begin{bmatrix} 0 & 1 & 0 \\ -1 & 0 & 0 \\ 0 & 0 & 0 \end{bmatrix}. \tag{C 1}$$

Therefore we find

$$\frac{\mathrm{d}}{\mathrm{d}\xi}|X|^2 = \mathrm{i}\frac{\Omega_0 L}{C_{\mathrm{g}}}(1+\tfrac{1}{2}\cos\psi)(TS^*-ST^*), \tag{C 2}$$

where both left- and right-hand sides are real. To evaluate the right-hand side, we multiply both sides of the first row of (7.6) by $(\frac{1}{2}\cos\psi S^* + (\Omega/\Omega_0)T^*)$ to get

$$\left(\tfrac{1}{2}\cos\psi S^* + \frac{\Omega}{\Omega_0}T^*\right)\frac{\mathrm{d}T}{\mathrm{d}\xi} = \mathrm{i}\frac{\Omega_0 L}{C_{\mathrm{g}}}\left[\frac{1}{2}\frac{\Omega}{\Omega_0}\cos\psi(TS^*-ST^*) - \tfrac{1}{4}\cos^2\psi|S|^2 + \left(\frac{\Omega}{\Omega_0}\right)^2|T|^2\right]. \tag{C 3}$$

Taking only the real part, we find

$$\tfrac{1}{4}\cos\psi\left(S^*\frac{\mathrm{d}T}{\mathrm{d}\xi}+S\frac{\mathrm{d}T^*}{\mathrm{d}\xi}\right)+\frac{1}{2}\frac{\Omega}{\Omega_0}\left(T^*\frac{\mathrm{d}T}{\mathrm{d}\xi}+T\frac{\mathrm{d}T^*}{\mathrm{d}\xi}\right) = \tfrac{1}{2}\mathrm{i}\cos\psi\frac{\Omega_0 L}{C_{\mathrm{g}}}\frac{\Omega}{\Omega_0}(TS^*-ST^*). \tag{C 4}$$

Since from the first row of (7.6) we can show that

$$\left(S^*\frac{\mathrm{d}T}{\mathrm{d}\xi}+S\frac{\mathrm{d}T^*}{\mathrm{d}\xi}\right) = \mathrm{i}\frac{\Omega_0 L}{C_{\mathrm{g}}}\frac{\Omega}{\Omega_0}(TS^*-ST^*) \tag{C 5}$$

it follows from (C 4) that

$$\frac{\mathrm{d}}{\mathrm{d}\xi}|T|^2 = \tfrac{1}{2}\mathrm{i}\cos\psi\frac{\Omega_0 L}{C_{\mathrm{g}}}(TS^*-ST^*). \tag{C 6}$$

Finally, upon combining (C 2) and (C 6), we obtain

$$\frac{\mathrm{d}}{\mathrm{d}\xi}[\tfrac{1}{2}\cos\psi\,|X|^2-(1+\tfrac{1}{2}\cos\psi)\,|T|^2]=\frac{\mathrm{d}}{\mathrm{d}\xi}[\tfrac{1}{2}\cos\psi\,(|S|^2+|D|^2)-|T|^2]=0 \qquad \text{(C 7)}$$

Integrating (C 7) from $\xi = 0$ to $\xi = 1$ and using the boundary conditions, we find

$$\tfrac{1}{2}\cos\psi\,(|S|^2+|D|^2)+|T|^2=1. \qquad \text{(C 8)}$$

Upon expressing S and D in terms of R_1 and R_2, we finally get

$$\cos\psi\,(|R_1|^2+|R_2|^2)+|T|^2=1. \qquad \text{(C 9)}$$

This result states the conservation of energy flux in the x-direction.

REFERENCES

Dalrymple, R. A. & Kirby, J. T. 1986 Water waves over ripples. *J. Waterways, Port, Coastal Ocean Engng* **112**, No. 2, 309–319.

Davies, A. G. & Heathershaw, A. D. 1984 Surface-wave propagation over sinusoidally varying topography. *J. Fluid Mech.* **144**, 419–443.

Hara, T. & Mei, C. C. 1987 Bragg scattering of surface waves by periodic bars – theory and experiment. *J. Fluid Mech.* **178**, 221–241.

Kirby, J. T. 1986 A general wave equation for waves over rippled beds. *J. Fluid Mech.* **162**, 171–196.

MaCabe, C. 1986 How Phillips is dealing with subsidence at Ekofisk. *Ocean Indust.* February, 30–34.

Mei, C. C. 1985 Resonant reflection of surface waves by periodic sandbars. *J. Fluid Mech.* **152**, 315–335.

Mitra, A. & Greenberg, M. D. 1984 Slow interaction of gravity waves and a corrugated seabed. *Trans. ASME.* E: *J. Appl. Mech.* **51**, 251–255.